

Supplementary data for the article: Ristić, P.; Blagojević, V.; Janjić, G.; Rodić, M.; Vulić, P.; Donnard, M.; Gulea, M.; Chylewska, A.; Makowski, M.; Todorović, T.; Filipović, N. Influence of C–H/X (X = S, Cl, N, Pt/Pd) Interactions on the Molecular and Crystal Structures of Pt(II) and Pd(II) Complexes with Thiomorpholine-4-Carbonitrile: Crystallographic, Thermal, and DFT Study. *Crystal Growth & Design* 2020, 20 (5), 3018–3033. <https://doi.org/10.1021/acs.cgd.9b01661>



This work is licensed under the [Creative Commons - Attribution 4.0 International \(CC BY 4.0\) license](https://creativecommons.org/licenses/by/4.0/)

## SUPPORTING INFORMATION

### **Influence of C–H/X (X = S, Cl, N, Pt/Pd) interactions on the molecular and crystal structures of Pt(II) and Pd(II) complexes with thiomorpholine-4-carbonitrile: crystallographic, thermal and DFT study**

Predrag Ristić<sup>a</sup>, Vladimir Blagojević<sup>b</sup>, Goran Janjić<sup>c</sup>, Marko Rodić<sup>d</sup>, Predrag Vulić<sup>e</sup>,  
Morgan Donnard<sup>f</sup>, Mihaela Gulea<sup>g</sup>, Agnieszka Chylewska<sup>h</sup>, Mariusz Makowski<sup>h</sup>,  
Tamara Todorović<sup>a</sup>, Nenad Filipović<sup>i,\*</sup>

<sup>a</sup> *University of Belgrade - Faculty of Chemistry, Studentski trg 12-16, 11000 Belgrade, Serbia*

<sup>b</sup> *Institute of Technical Sciences of the Serbian Academy of Sciences and Arts, Knez Mihailova 35/IV, 11000 Belgrade, Serbia*

<sup>c</sup> *Institute of Chemistry, Metallurgy and Technology, University of Belgrade, Njegoševa 12, 11000 Belgrade, Serbia*

<sup>d</sup> *Department of Chemistry, Faculty of Sciences, University of Novi Sad, Trg Dositeja Obradovića 4, 21000 Novi Sad, Serbia*

<sup>e</sup> *Faculty of Mining and Geology, University of Belgrade, Dušina 5, 11000 Belgrade, Serbia*

<sup>f</sup> *Université de Strasbourg, Université de Haute-Alsace, CNRS, LIMA – UMR 7042, ECPM, 67000 Strasbourg, France*

<sup>g</sup> *Université de Strasbourg, CNRS, LIT – UMR 7200, Faculty of Pharmacy, 67000 Strasbourg, France*

<sup>h</sup> *Faculty of Chemistry, University of Gdansk, Wita Stwosza 63, PL80-308 Gdansk, Poland*

<sup>i</sup> *University of Belgrade - Faculty of Agriculture, Nemanjina 6, 11000 Belgrade, Serbia*

\*Corresponding author: Nenad Filipović, PhD, Associate Professor, University of Belgrade - Faculty of Agriculture, Nemanjina 6, 11000 Belgrade, Serbia; E-mail: nenadf@agrif.bg.ac.rs

## SUPPLEMENTARY FIGURES AND SCHEMES

**Figure S1.** IR spectra of gaseous decomposition products obtained during TG experiments with **1**(A) and **2** (B).

**Figure S2.** The 3D presentation of thermal decompositions *versus* time together with IR spectra of their gaseous products: (a) **1**; (b) **2**.

**Figure S3.** Overlapped experimental (blue) and calculated (red) powder XRD diffractograms of **1** (A) and **2** (B).

**Figure S4.** Comparison between experimental powder XRD patterns of **1** (left) and **2** (right) with simulated patterns of their analogues with different position of M–S bond with respect to the TM-CN ring chair conformation.

**Figure S5.** Optical microscope images of Pt- (left) and Pd-complex (right) showing as-obtained single crystals.

**Figure S6.** SEM images of Pt- (left) and Pd-complex (right) after reduction to powder for XRD measurements.

**Figure S7.**  $^1\text{H}$  NMR spectra of TM-CN in DMSO- $d_6$  (A) and  $\text{CD}_3\text{NO}_2$  (B).

**Figure S8.**  $^{13}\text{C}$  NMR spectra of TM-CN in DMSO- $d_6$  (A) and  $\text{CD}_3\text{NO}_2$  (B).

**Figure S9.**  $^1\text{H}$  (A) and  $^{13}\text{C}$  NMR (B) spectra of **1** in DMSO- $d_6$ .

**Figure S10.** COSY spectrum of **1** in DMSO- $d_6$ .

**Figure S11.** NOESY spectrum of **1** in DMSO- $d_6$ .

**Figure S12.**  $^1\text{H}$ – $^{13}\text{C}$  HSQC spectrum of **1** in DMSO- $d_6$ .

**Figure S13.**  $^1\text{H}$  (A) and  $^{13}\text{C}$  NMR (B) spectra of **1** in  $\text{CD}_3\text{NO}_2$ .

**Figure S14.**  $^1\text{H}$  (A) and  $^{13}\text{C}$  NMR (B) spectra of **2** in DMSO- $d_6$ .

**Figure S15.**  $^1\text{H}$  (A) and  $^{13}\text{C}$  NMR (B) spectra of **2** in  $\text{CD}_3\text{NO}_2$ .

**Scheme S1.** Labelling of atoms used for NMR signal assignments.

## SUPPLEMENTARY TABLES

**Table S1.** Experimental vibrational frequencies ( $\text{cm}^{-1}$ ) and signals description of complexes studied.

**Table S2.** Crystal data and structure refinement for **1** and **2**.

**Table S3.** Selected bond lengths ( $\text{\AA}$ ) and angles ( $^\circ$ ) for complexes **1** and **2**.

**Table S4.** Results of energy calculations for C-H/Cl-M, C-H/S-M, C-H/M and C-H/N $\equiv$ C interactions (M= Pd(II) and Pt(II)) at *wb97xd/6-31+g\*\* +lanl2dz* level of theory. Energies are expressed in kcal/mol.

**Table S5.** C-H/M interactions obtained from the periodic calculations of axial and equatorially coordinated Pd and Pt.

**Table S6.**  $^1\text{H}$  NMR spectral data (399.74 MHz) in DMSO-*d*<sub>6</sub> and CD<sub>3</sub>NO<sub>2</sub> at 298 K for TM-CN and complexes **1** and **2**.

**Table S7.**  $^{13}\text{C}$  NMR spectral data (100.53 MHz) in DMSO-*d*<sub>6</sub> and CD<sub>3</sub>NO<sub>2</sub> at 298 K for TM-CN and complexes **1** and **2**.

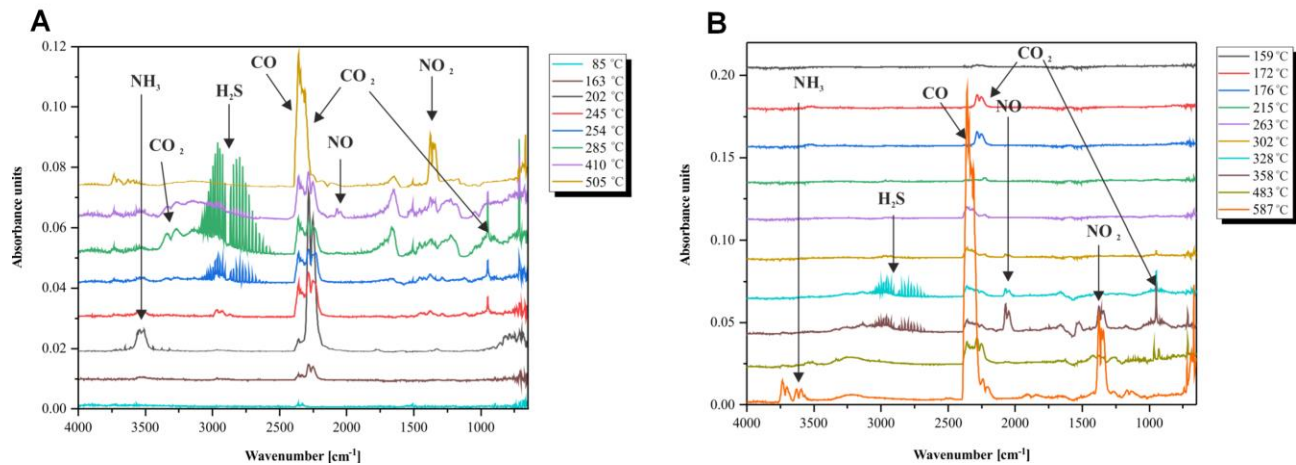


**Figure S1.** IR spectra of gaseous decomposition products obtained during TG experiments with **1**(A) and **2** (B).

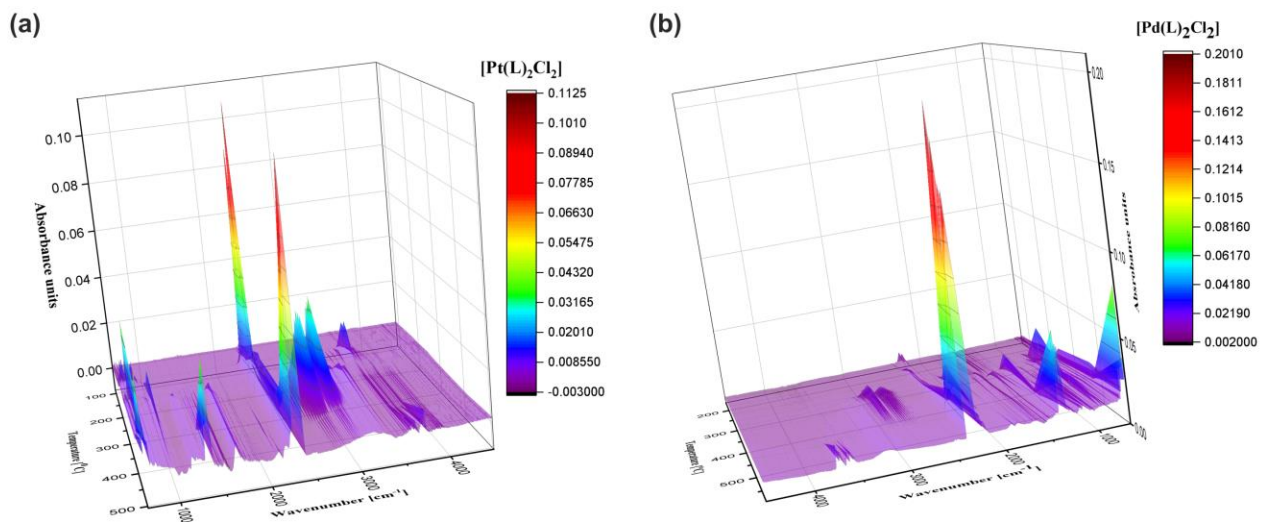


**Figure S2.** The 3D presentation of thermal decompositions vs time together with IR spectra of their gaseous products: (a) **1**; (b) **2**.

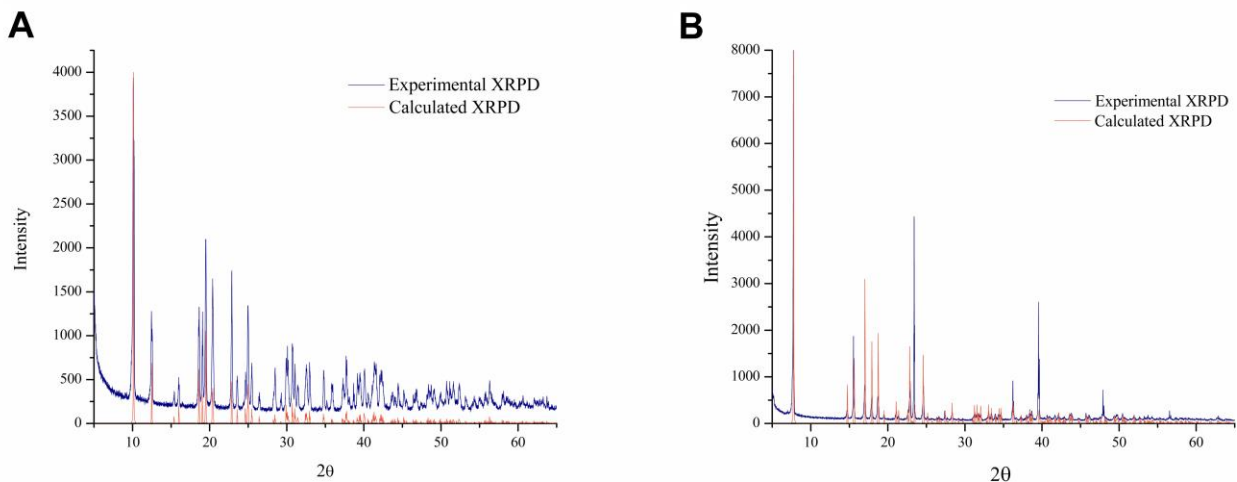


**Figure S3.** Overlapped experimental (blue) and calculated (red) powder XRD diffractograms of **1** (A) and **2** (B).

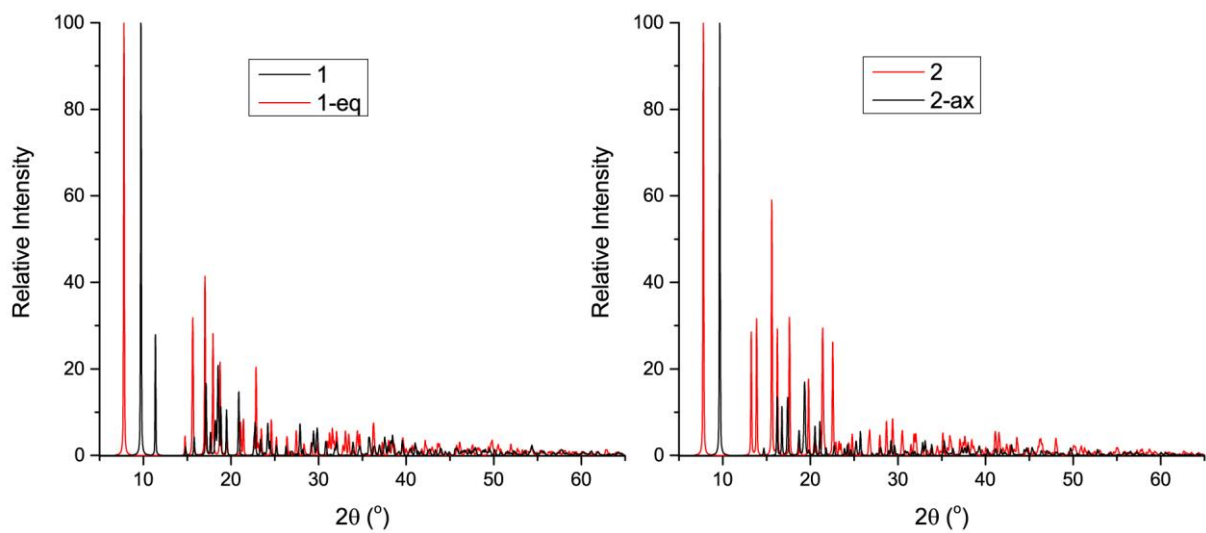


**Figure S4.** Comparison between experimental powder XRD patterns of **1** (left) and **2** (right) with simulated patterns of their analogues with different TM-CN conformation of metal-sulfur bond.

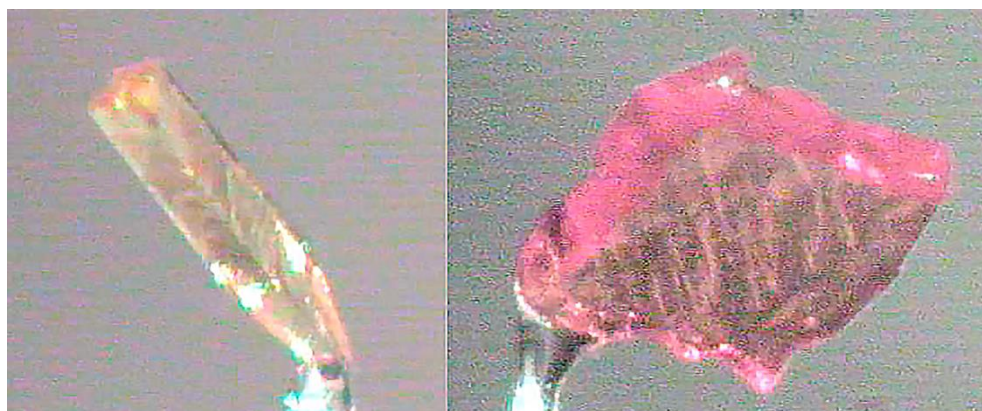


**Figure S5.** Optical microscope images of Pt- (left) and Pd-complex (right) showing as-obtained single crystals.

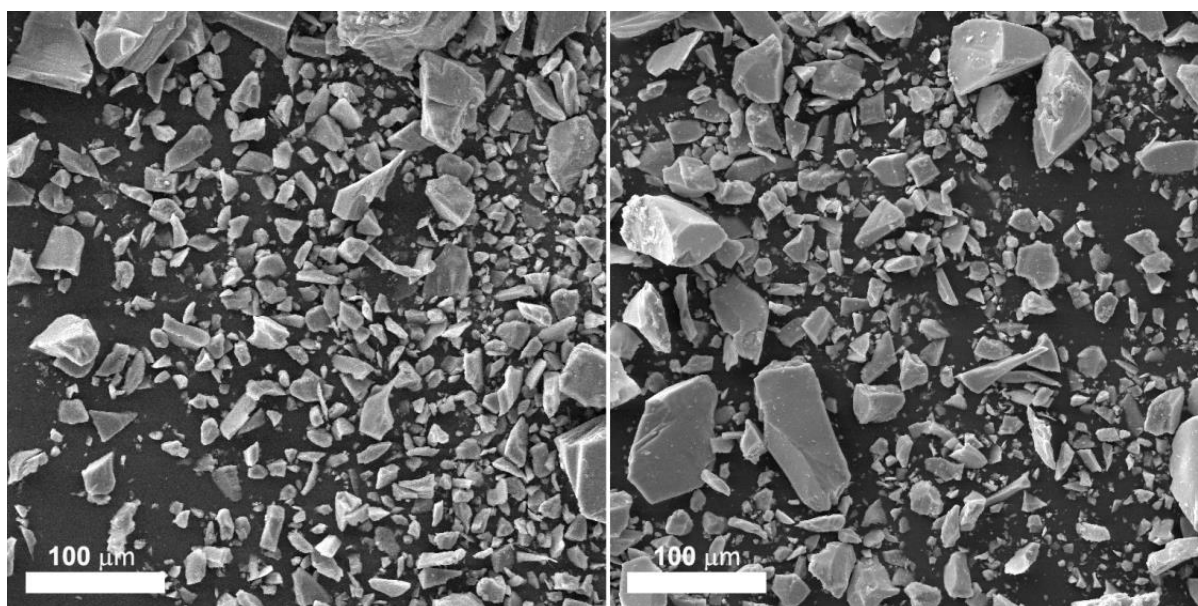


**Figure S6.** SEM images of Pt- (left) and Pd-complex (right) after reduction to powder for XRD measurements.

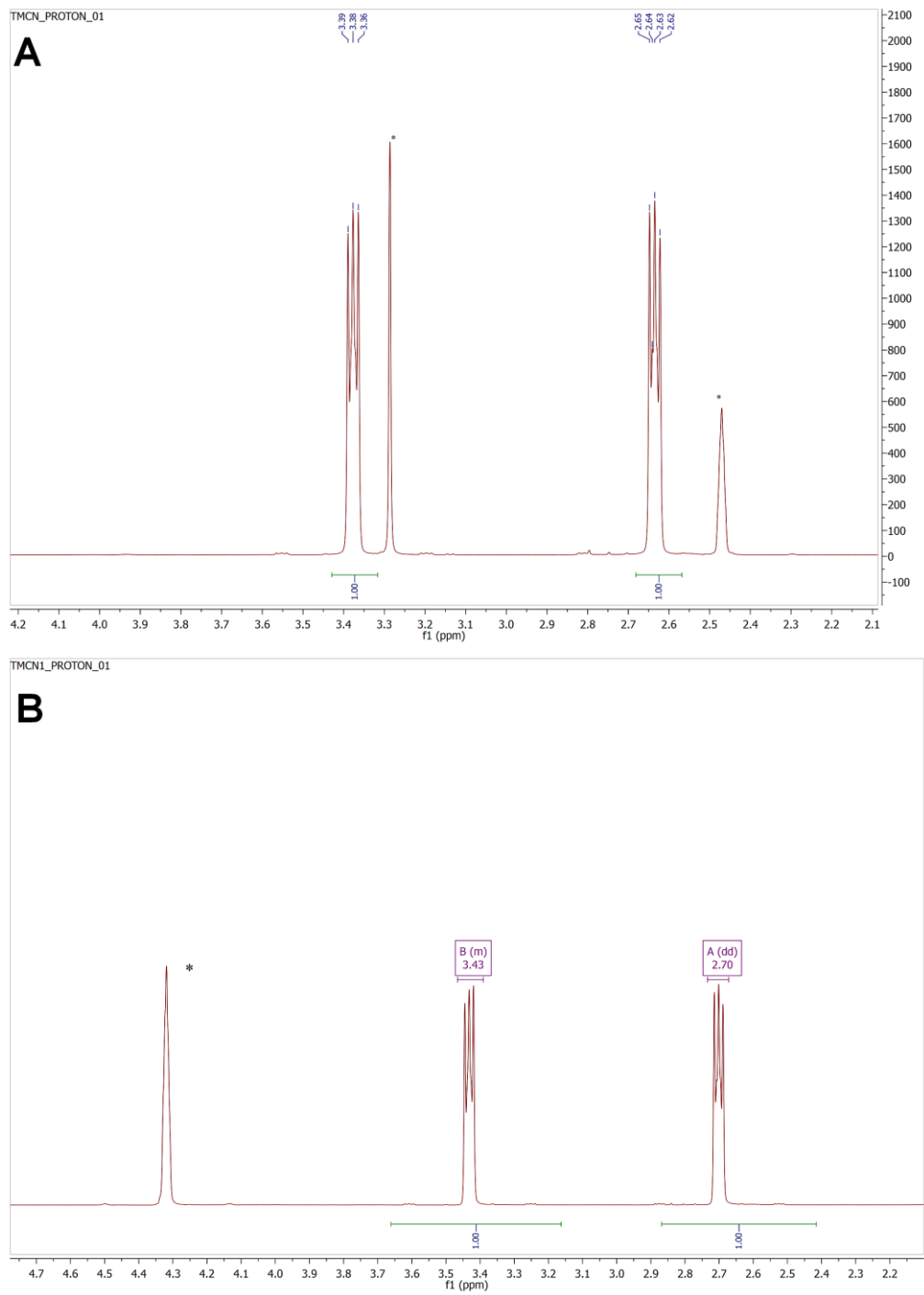


**Figure S7.**  $^1\text{H}$  NMR spectra of TM-CN in  $\text{DMSO-}d_6$  (A) and  $\text{CD}_3\text{NO}_2$  (B).



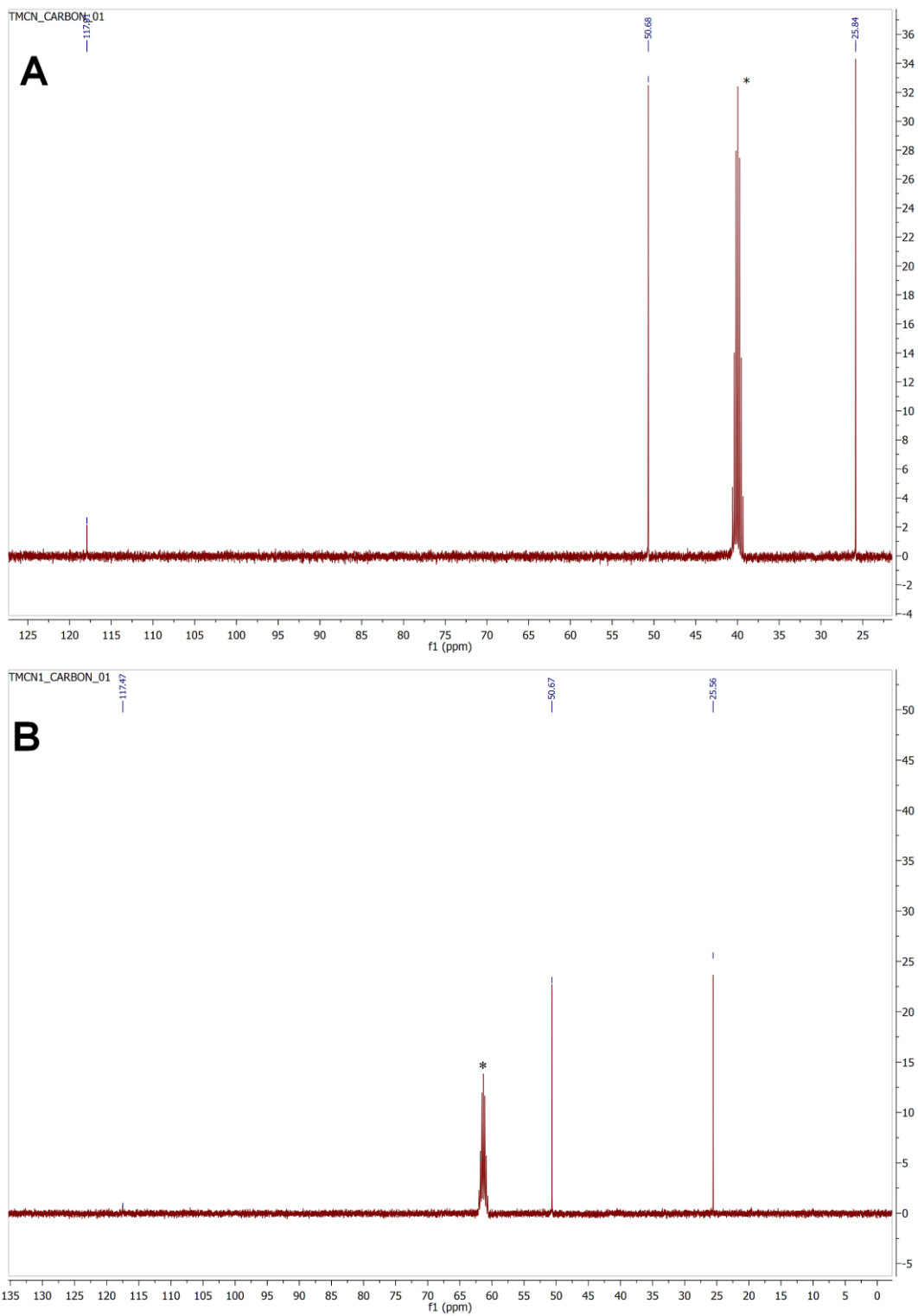


**Figure S8.**  $^{13}\text{C}$  NMR spectra of TMCN in  $\text{DMSO-}d_6$  (A) and  $\text{CD}_3\text{NO}_2$  (B).

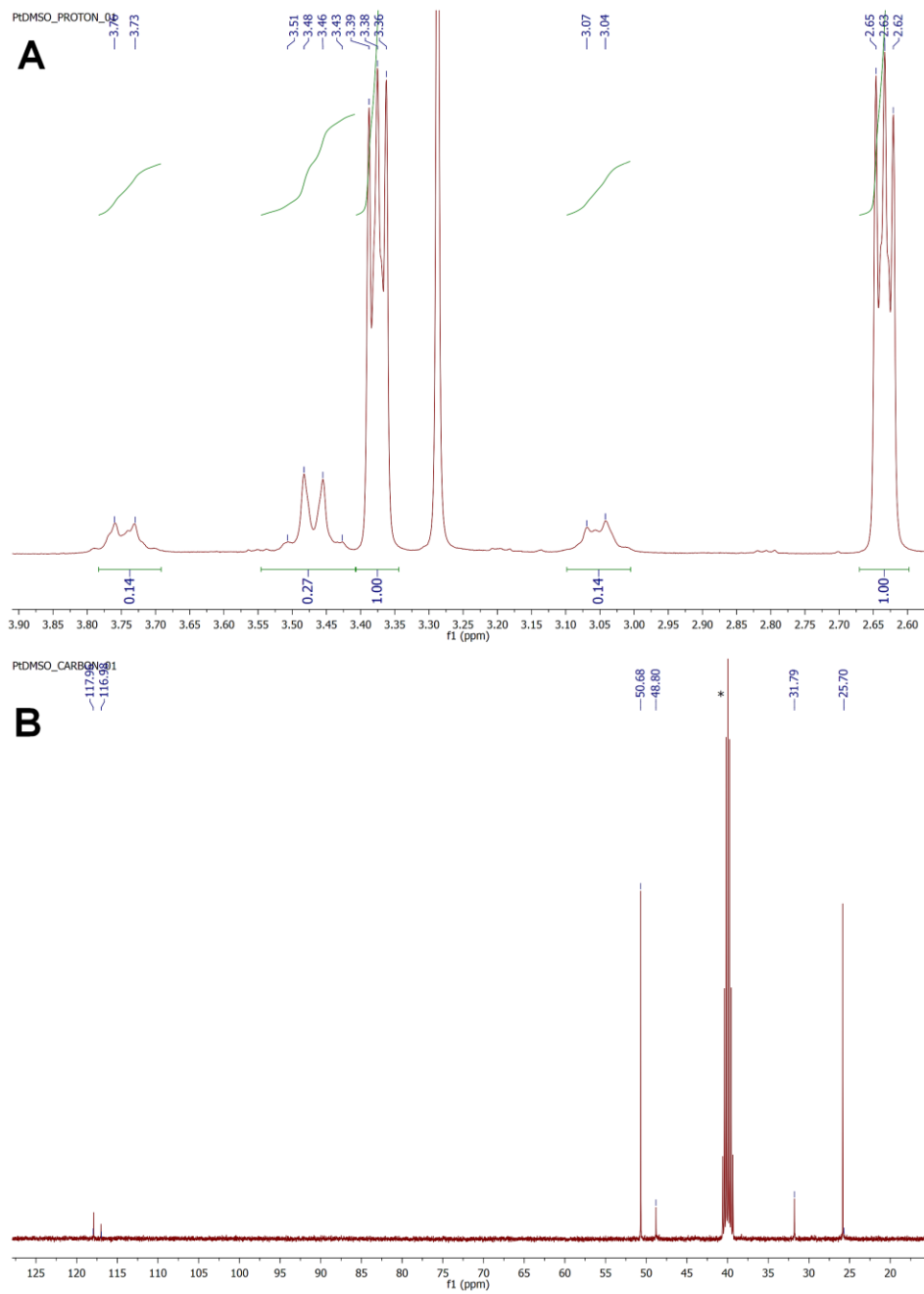


**Figure S9.**  $^1\text{H}$  (A) and  $^{13}\text{C}$  NMR (B) spectra of **1** in  $\text{DMSO-}d_6$ .

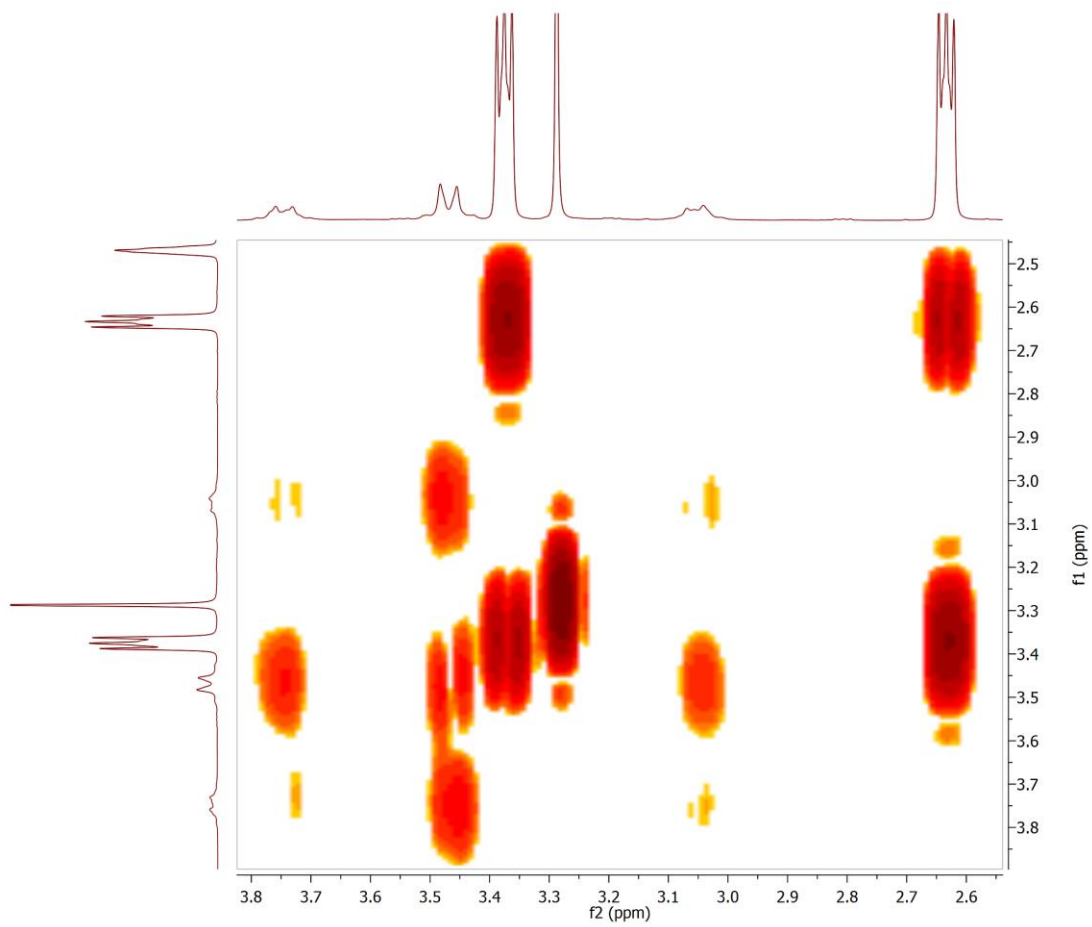


**Figure S10.** COSY spectrum of **1** in DMSO- $d_6$ .

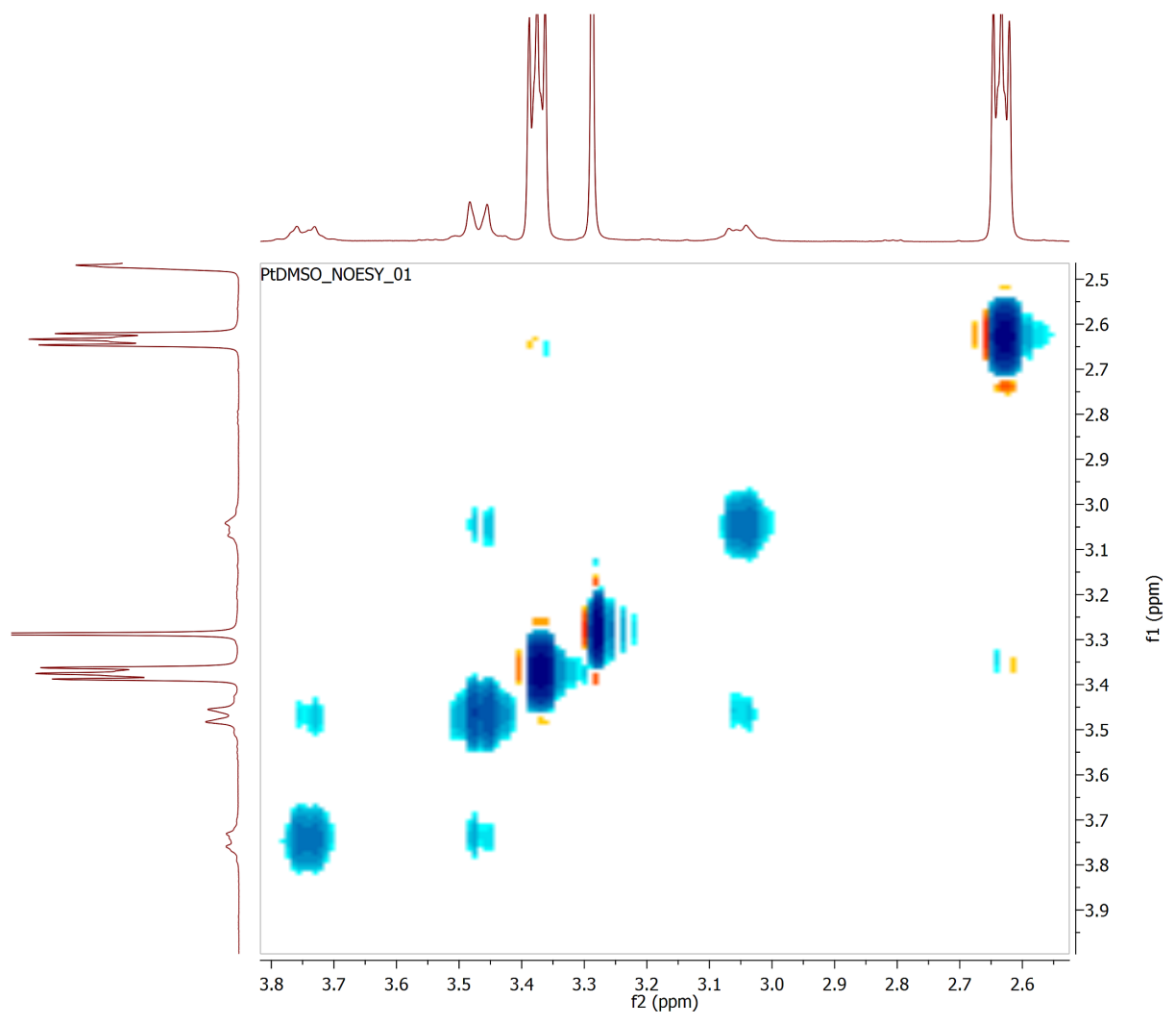


**Figure S11.** NOESY spectrum of **1** in DMSO-*d*<sub>6</sub>.

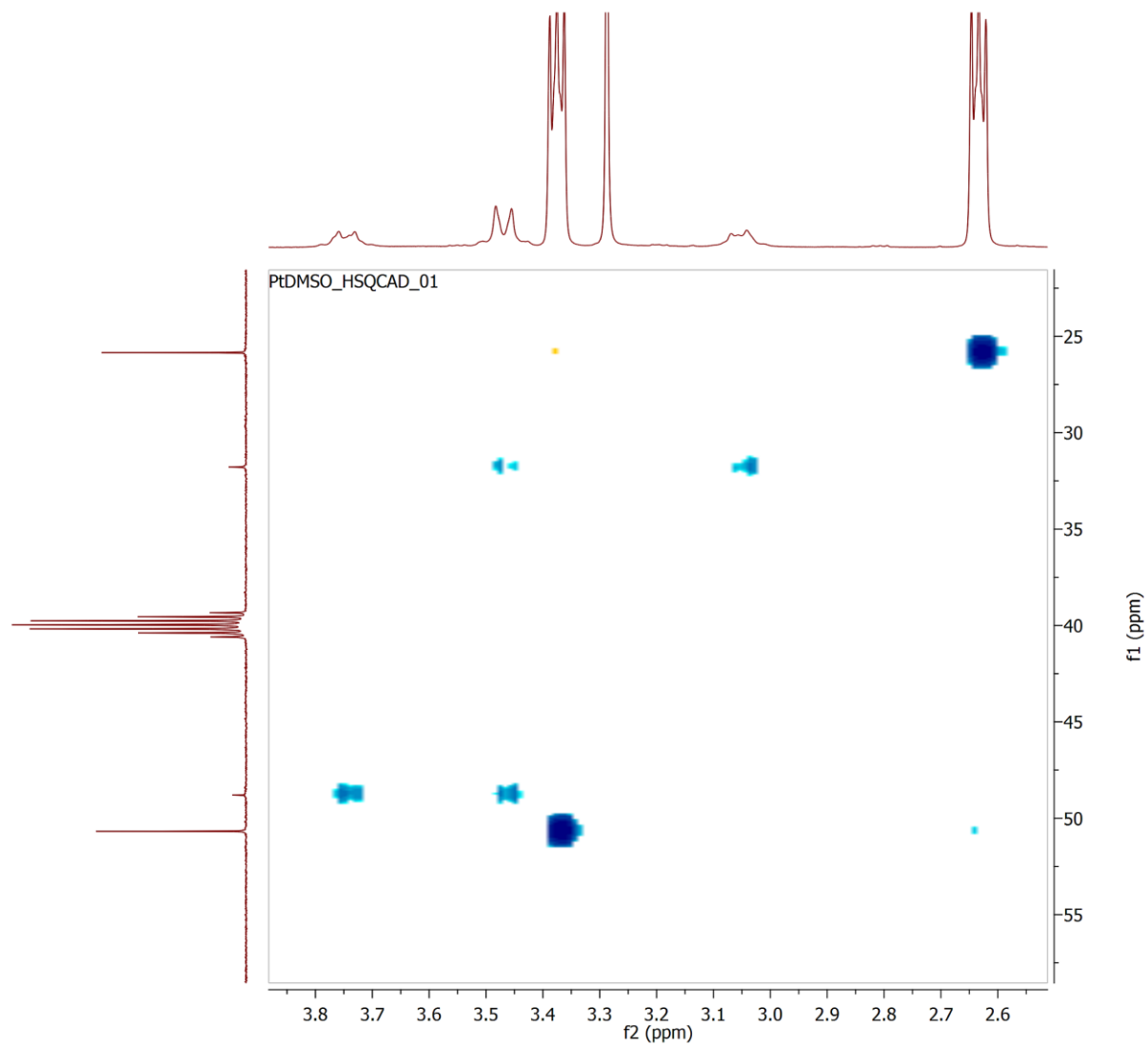


**Figure S12.**  $^1\text{H}$ - $^{13}\text{C}$  HSQC spectrum of **1** in  $\text{DMSO-}d_6$ .

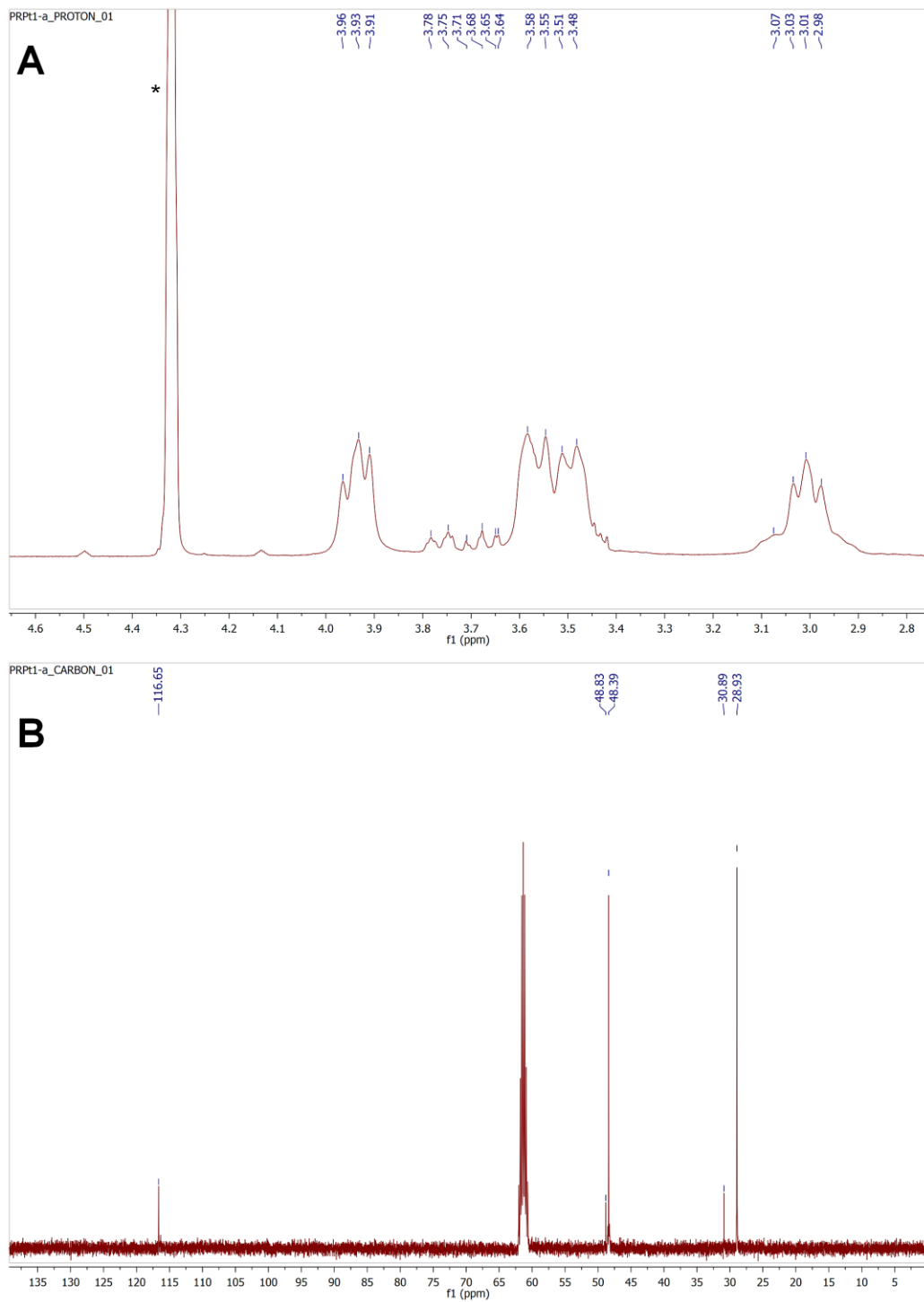


**Figure S13.**  $^1\text{H}$  (A) and  $^{13}\text{C}$  NMR (B) spectra of **1** in  $\text{CD}_3\text{NO}_2$ .

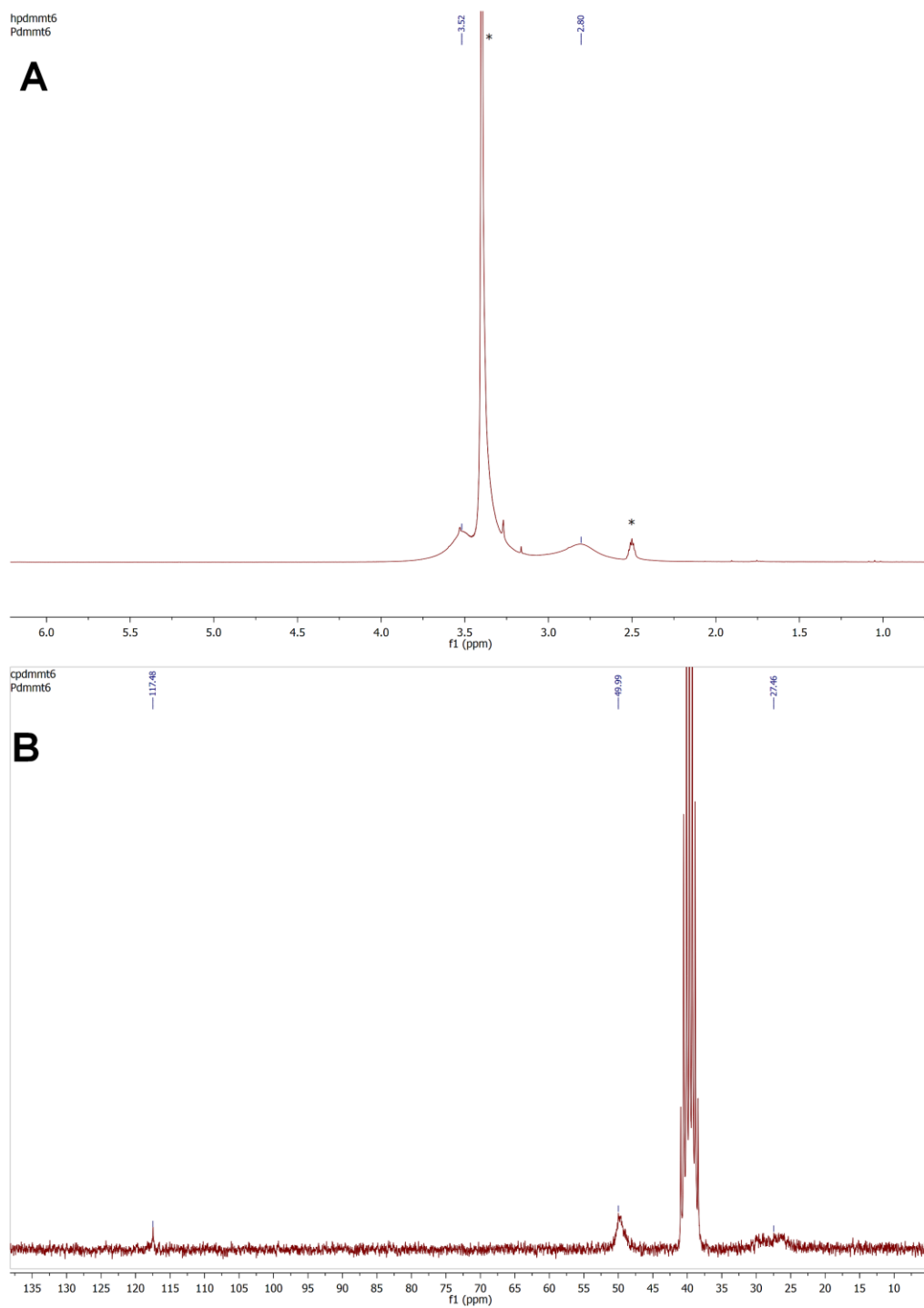


**Figure S14.**  $^1\text{H}$  (A) and  $^{13}\text{C}$  NMR (B) spectra of **2** in  $\text{DMSO-}d_6$ .

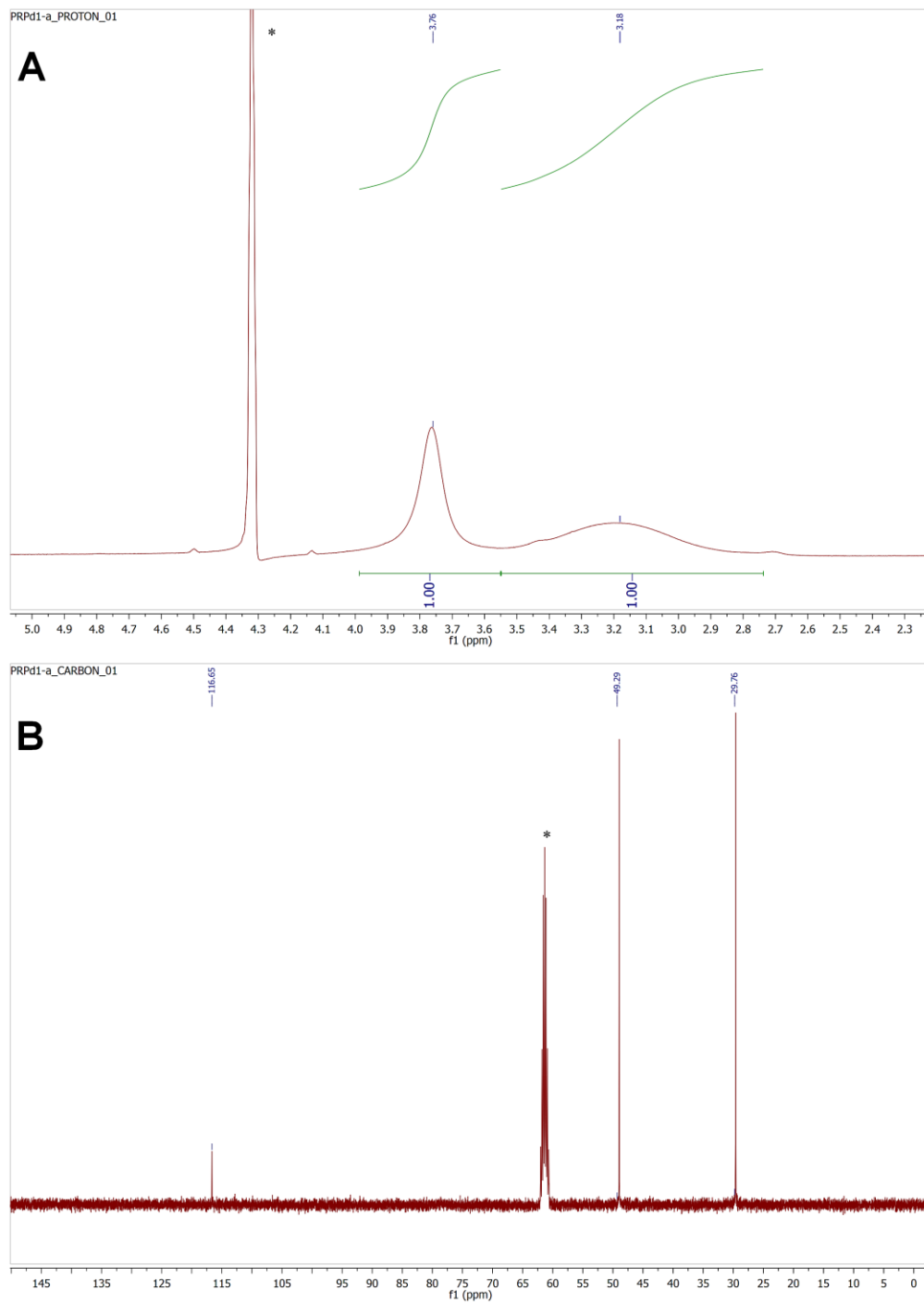


**Figure S15.**  $^1\text{H}$  (A) and  $^{13}\text{C}$  NMR (B) spectra of **2** in  $\text{CD}_3\text{NO}_2$ .



**Table S1.** Experimental vibrational frequencies ( $\text{cm}^{-1}$ ) and signals description of complexes studied.

1			2			
UATR experimental frequency ( $\text{cm}^{-1}$ )	IR intensity (%)	Vibrational assignments	UATR experimental frequency ( $\text{cm}^{-1}$ )	IR intensity (%)	Vibrational assignments	
3601 vw	(92)	<i>trans</i> - geometry	3461 vw	(93)	<i>trans</i> - geometry	
3355 w	(92)		3354 w	(93)		
2997 w	(91)	CH <sub>2</sub> sym	2995 ms	(90)	CH <sub>2</sub> sym	
2980 w	(89)		2925 vw	(93)	CH <sub>2</sub> asym	
2916 vw	(91)		CH <sub>2</sub> asym	2263 ms	(88)	v C≡N
2867 vw	(91)			2214 s	(80)	
2208 vs	(59)	v C≡N	1649 ms	(89)	v C-S	
1652 w	(93)	v C-S	1597 ms	(89)		
1598 w	(92)		1546 ms	(91)		
1454 s	(82)		1401 s	(81)		
1420 s	(79)		1277 s	(84)		
1391 s	(74)	v C-C CH <sub>2</sub> wag CH <sub>2</sub> twist	1197 mw	(88)	v C-C	
1364 s	(78)		1166 mw	(86)	CH <sub>2</sub> wag	
1283 s	(82)		1113 mw	(87)	CH <sub>2</sub> twist	
1227 ms	(87)		1029 s	(85)	b C≡N	
1197 ms	(87)		946 vs	(67)	CH <sub>2</sub> rock	
1176 ms	(83)		832 w	(91)		
1147 ms	(82)		734 mw	(89)		
1120 s	(78)		648 mw	(89)		
1027 s	(79)	b C≡N	573 mw	(86)		
980 ms	(83)	CH <sub>2</sub> rock	543 mw	(85)	b NCN	

1			2		
UATR experimental frequency (cm <sup>-1</sup> )	IR intensity (%)	Vibrational assignments	UATR experimental frequency (cm <sup>-1</sup> )	IR intensity (%)	Vibrational assignments
949 vs	(56)		504 s	(79)	v Pd-S
726 ms	(88)		374 vw	(90)	v Pd-Cl
580 s	(84)		364 w	(84)	
540 ms	(88)	b NCN	355 vs	(56)	
505 vs	(74)	v Pt-S	333 s	(78)	
354 vs	(53)	v Pt-Cl	319 vs	(28)	
347 vs	(25)				
339 vs	(10)				
321 vs	(22)				

*Abbreviations used:* v = stretching; b = bending; wag = wagging; twist = twisting; rock = rocking; sym = symmetric stretch; asym = asymmetric stretch; w = weak; m = medium; s = strong; ms = medium strong; vs = very strong; vw = very weak.

**Table S2.** Crystal data and structure refinement for **1** and **2**.

Compound	<b>1</b>	<b>2</b>
Molecular formula	C <sub>10</sub> H <sub>16</sub> Cl <sub>2</sub> N <sub>4</sub> PtS <sub>2</sub>	C <sub>10</sub> H <sub>16</sub> Cl <sub>2</sub> N <sub>4</sub> PdS <sub>2</sub>
Formula weight	522.38	433.69
Temperature (K)	294(2)	294(2)
Wavelength (Å)	0.71073	0.71073
Crystal system	Monoclinic	Monoclinic
Space group	<i>I</i> 2/ <i>a</i>	<i>P</i> 2 <sub>1</sub> / <i>c</i>
<i>a</i> (Å)	9.9954(3)	11.4399(4)
<i>b</i> (Å)	11.0764(3)	7.0711(2)
<i>c</i> (Å)	14.8663(4)	9.5192(4)
β (°)	107.508(3)	96.179(4)
Volume (Å <sup>3</sup> )	1569.64(7)	765.56(5)
<i>Z</i>	4	2
ρ <sub>calc</sub> (Mg/m <sup>3</sup> )	2.211	1.881
μ (mm <sup>-1</sup> )	9.537	1.82
<i>F</i> (000)	992	432
Crystal size (mm)	0.61 × 0.14 × 0.11	0.51 × 0.49 × 0.14
θ Range for data collection (°)	2.33 – 28.93	3.39 – 29.06
Reflections collected	7449	25252
Independent reflections	1903 [ <i>R</i> (int) = 0.046]	3440 [ <i>R</i> (int) = 0.070]
Absorption correction	Gaussian	Analytical
Refinement method	full-matrix least-squares on <i>F</i> <sup>2</sup>	
Data/restraints/parameters	1903/0/89	3440/0/90
Goodness-of-fit on <i>F</i> <sup>2</sup>	1.27	1.25
Final <i>R</i> indexes [ <i>I</i> > 2σ( <i>I</i> )]	<i>R</i> <sub>1</sub> = 0.0327, <i>wR</i> <sub>2</sub> = 0.0802	<i>R</i> <sub>1</sub> = 0.0505, <i>wR</i> <sub>2</sub> = 0.1176
Final <i>R</i> indexes [all data]	<i>R</i> <sub>1</sub> = 0.0387, <i>wR</i> <sub>2</sub> = 0.0835	<i>R</i> <sub>1</sub> = 0.0551, <i>wR</i> <sub>2</sub> = 0.1211
Largest diff. peak and hole, e Å <sup>-3</sup>	1.06 and -2.18	1.30 and -1.66

**Table S3.** Selected bond lengths (Å), bond angles (°) and torsional angles (°) for complexes **1** and **2**.

	<b>1</b>	<b>2</b>
M1 <sup>a</sup> -Cl1	2.3059(11)	2.2981(9)
M1-S1	2.3135(10)	2.3121(9)
S1-C1	1.816(5)	1.823(4)
S1-C3	1.810(5)	1.808(4)
N1-C2	1.463(6)	1.471(6)
N1-C5	1.315(6)	1.317(6)
N1-C4	1.454(6)	1.452(6)
Cl1-M1-S1 <sup>i</sup>	86.43(4)	95.34(3)
Cl1-M1-Cl1 <sup>i</sup>	180	180
S1-M1-Cl1	93.57(4)	84.66(3)
S1-M1-S1 <sup>i</sup>	180	180
C5-N1-C4	118.1(4)	121.7(4)
C5-N1-C2	118.1(4)	119.2(4)
C4-N1-C2	117.6(4)	118.2(3)
M1 <sup>a</sup> -S1-C1-C2	60.89	172.48
M1 <sup>a</sup> -S1-C3-C4	59.80	167.98

<sup>a</sup> M = Pt in **1**; M = Pd in **2**.

*i* = 1 - *x*, 1 - *y*, 1 - *z* in **1**;

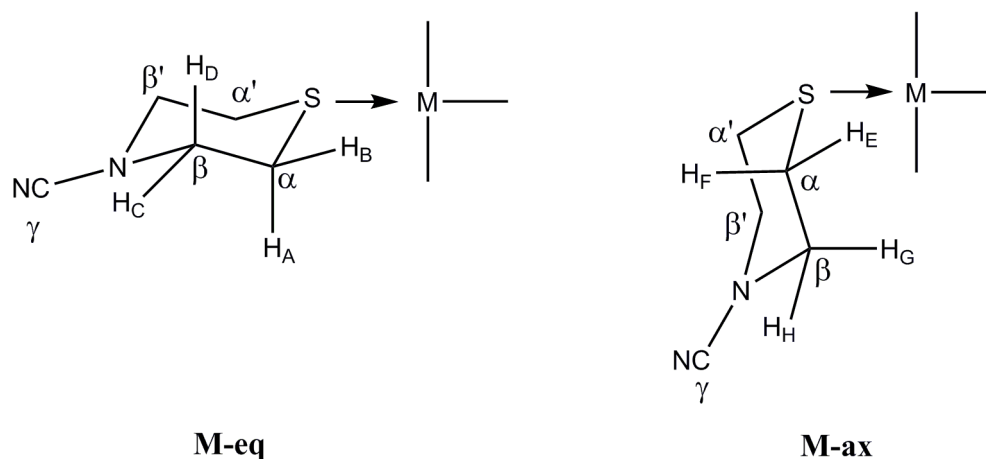
*i* = 1 - *x*, -*y*, 1 - *z* in **2**

**Table S4.** Results of energy calculations for C–H/Cl–M, C–H/S–M, C–H/M and C–H/N≡C interactions (M = Pd, Pt) at *wb97xd/6-31+g\*\* +lanl2dz* level of theory. Energies are expressed in kcal/mol.

d	C–H/ Cl–Pd	C–H/ Cl–Pt	C–H/ S–Pd	C–H/ S–Pt	C–H/ Pd	C–H/ Pt	C–H/NC (Pd)	C–H/NC (Pt)
2.50	0.09	0.06	0.85	0.56	–2.21	–1.82	–0.39	–0.39
2.70	–0.42	–0.44	–0.20	–0.44	–2.78	–2.70	–0.56	–0.56
2.80	–0.54	–0.55	–0.47	–0.69	–2.84	–2.88	–0.57	–0.57
2.90	–0.59	–0.60	–0.63	–0.83	–2.80	–2.95	–0.56	–0.56
3.00	–0.60	–0.62	–0.72	–0.90	–2.71	–2.93	–0.54	–0.54
3.20	–0.58	–0.59	–0.75	–0.90	–2.43	–2.72	–0.48	–0.48
3.50	–0.46	–0.49	–0.65	–0.76	–1.92	–2.21	–0.39	–0.39

**Table S5.** C–H/M interactions obtained from the periodic calculations of axial and equatorially coordinated Pd and Pt.

Complex	Number of C–H/M interactions	C–H/M distances (Å)
2	4	3.785, 4.050, 4.481, 4.933
1	5	3.326, 3.955, 4.798, 4.863, 5.892
2-ax	5	3.719, 4.681, 4.683, 5.164, 5.643
1-eq	4	3.682, 4.058, 4.478, 4.974



**Scheme S1.** Labelling of atoms used for NMR signal assignments. M = Pt in **1**; M = Pd in **2**.

**Table S6.**  $^1\text{H}$  NMR spectral data (399.74 MHz) in  $\text{DMSO-}d_6$  and  $\text{CD}_3\text{NO}_2$  at 298 K for TM-CN and complexes **1** and **2**.

	$\text{DMSO-}d_6$	$\text{CD}_3\text{NO}_2$
TM-CN	$\delta$ 3.40 – 3.36 (m, 4H, $\text{C}^\beta\text{H}_2 = \text{C}^{\beta'}\text{H}_2$ ), 2.64 (dd, $J = 6.2, 3.9$ Hz, 4H, $\text{C}^\alpha\text{H}_2 = \text{C}^{\alpha'}\text{H}_2$ ).	$\delta$ 3.47 – 3.39 (m, 4H, $\text{C}^\beta\text{H}_2 = \text{C}^{\beta'}\text{H}_2$ ), 2.70 (dd, $J = 6.2, 3.9$ Hz, 4H, $\text{C}^\alpha\text{H}_2 = \text{C}^{\alpha'}\text{H}_2$ ).
<b>1</b>	<b>1-ax</b> (minor): $\delta$ 3.75 (br. d, $J = 12.1$ Hz, 2H, $\text{C}^\beta\text{H}_D = \text{C}^{\beta'}\text{H}_{D'}$ ), 3.50 (br. s, 2H, $\text{C}^\beta\text{H}_C = \text{C}^{\beta'}\text{H}_{C'}$ ), 3.46 (br. s, 2H, $\text{C}^\alpha\text{H}_B = \text{C}^{\alpha'}\text{H}_{B'}$ ), 3.06 (br. d, $J = 10.9$ Hz, 1H, $\text{C}^\alpha\text{H}_A = \text{C}^{\alpha'}\text{H}_{A'}$ ).	<b>1-ax</b> (major): $\delta$ 3.93 (m, $\text{C}^\beta\text{H}_D = \text{C}^{\beta'}\text{H}_{D'}$ ), 3.56 (d, $J = 14.9$ Hz, $\text{C}^\beta\text{H}_C = \text{C}^{\beta'}\text{H}_{C'}$ ), 3.50 (d, $J = 12.1$ Hz, $\text{C}^\alpha\text{H}_B = \text{C}^{\alpha'}\text{H}_{B'}$ ), 3.01 (m, $\text{C}^\alpha\text{H}_A = \text{C}^{\alpha'}\text{H}_{A'}$ ).
	<b>TM-CN</b> (major): $\delta$ 3.38 (m, 4H, $\text{C}^\beta\text{H}_2 = \text{C}^{\beta'}\text{H}_2$ ), 2.63 (m, 4H, $\text{C}^\alpha\text{H}_2 = \text{C}^{\alpha'}\text{H}_2$ ).	<b>1-eq</b> (minor): $\delta$ 3.77 (d, $\text{C}^\beta\text{H}_C = \text{C}^{\beta'}\text{H}_{C'}$ ), 3.67 (m, $\text{C}^\alpha\text{H}_A = \text{C}^{\alpha'}\text{H}_{A'}$ ), 3.56 (ovlp., $\text{C}^\beta\text{H}_D = \text{C}^{\beta'}\text{H}_{D'}$ ), 3.07 (ovlp, $\text{C}^\alpha\text{H}_B = \text{C}^{\alpha'}\text{H}_{B'}$ ).
<b>2</b>	$\delta$ 3.52 (br. s, 4H, $\text{C}^\alpha\text{H}_2 = \text{C}^{\alpha'}\text{H}_2$ ), 2.80 (br. s, 4H, $\text{C}^\alpha\text{H}_2 = \text{C}^{\alpha'}\text{H}_2$ )	$\delta$ 3.76 (br. s, 4H, $\text{C}^\alpha\text{H}_2 = \text{C}^{\alpha'}\text{H}_2$ ), 3.18 (br. s, 4H, $\text{C}^\alpha\text{H}_2 = \text{C}^{\alpha'}\text{H}_2$ )

**Table S7.**  $^{13}\text{C}$  NMR spectral data (100.53 MHz) in  $\text{DMSO-}d_6$  and  $\text{CD}_3\text{NO}_2$  at 298 K for TM-CN and complexes **1** and **2**.

	$\text{DMSO-}d_6$	$\text{CD}_3\text{NO}_2$
TM-CN	$\delta$ 117.91 ( $\text{C}^\gamma$ ), 50.68 ( $\text{C}^\beta = \text{C}^{\beta'}$ ), 25.84 ( $\text{C}^\alpha = \text{C}^{\alpha'}$ ).	$\delta$ 117.47 ( $\text{C}^\gamma$ ), 50.67 ( $\text{C}^\beta = \text{C}^{\beta'}$ ), 25.56 ( $\text{C}^\alpha = \text{C}^{\alpha'}$ ).
<b>1</b>	<b>1-ax:</b> $\delta$ 116.98 ( $\text{C}^\gamma$ ), 48.80 ( $\text{C}^\beta = \text{C}^{\beta'}$ ), 31.79 ( $\text{C}^\alpha = \text{C}^{\alpha'}$ ).	<b>1-ax</b> (major): $\delta$ 116.65 ( $\text{C}^\gamma$ ), 48.39 ( $\text{C}^\beta = \text{C}^{\beta'}$ ), 28.93 ( $\text{C}^\alpha = \text{C}^{\alpha'}$ ).
	<b>TM-CN:</b> $\delta$ 117.96 ( $\text{C}^\gamma$ ), 50.68 ( $\text{C}^\beta = \text{C}^{\beta'}$ ), 25.70 ( $\text{C}^\alpha = \text{C}^{\alpha'}$ ).	<b>1-eq</b> (minor): $\delta$ 116.61 ( $\text{C}^\gamma$ ), 48.83 ( $\text{C}^\beta = \text{C}^{\beta'}$ ), 30.89 ( $\text{C}^\alpha = \text{C}^{\alpha'}$ ).
<b>2</b>	$\delta$ 117.48 ( $\text{C}^\gamma$ ), 49.99 ( $\text{C}^\beta = \text{C}^{\beta'}$ ), 27.46 ( $\text{C}^\alpha = \text{C}^{\alpha'}$ ).	$\delta$ 116.65 ( $\text{C}^\gamma$ ), 49.29 ( $\text{C}^\beta = \text{C}^{\beta'}$ ), 29.76 ( $\text{C}^\alpha = \text{C}^{\alpha'}$ ).